Earth Syst. Dynam. Discuss., 4, 1035–1064, 2013
www.earth-syst-dynam-discuss.net/4/1035/2013/
doi:10.5194/esdd-4-1035-2013

Earth System Dynamics Discussions
Open Access

Global soil organic carbon stock projection uncertainties relevant to sensitivity of global mean temperature and precipitation changes

K. Nishina[1], A. Ito[1], D. J. Beerling[6], P. Cadule[7], P. Ciais[7], D. B. Clark[4], P. Falloon[3], A. D. Friend[5], R. Kahana[3], E. Kato[1], R. Keribin[5], W. Lucht[2], M. Lomas[6], T. T. Rademacher[5], R. Pavlick[8], S. Schaphoff[2], N. Vuichard[7], L. Warszawaski[2], and T. Yokohata[1]

[1]National Institute for Environmental Studies, 16-2, Onogawa, Tsukuba, Ibaraki, Japan
[2]Potsdam Institute for Climate Impact Research, Telegraphenberg A 31, 14473, Potsdam, German
[3]Met Office Hadley Centre, FitzRoy Road, Exeter, Devon, EX1 3PB, UK
[4]Centre for Ecology and Hydrology, Wallingford, OX10 8BB, UK
[5]Department of Geography, University of Cambridge, Downing Place, Cambridge CB2 3EN, UK
[6]Department of Animal and Plant Sciences, University of Sheffield, Sheffield S10 2TN, UK
[7]Laboratoire des Sciences du Climat et de l'Environment, Joint Unit of CEA-CNRS-UVSQ, Gif-sur-Yvette, France

[8]Max Planck Institute for Biogeochemistry, Hans-Knöll-Str. 10, 07745 Jena, Germany

Received: 27 August 2013 – Accepted: 5 September 2013 – Published: 12 September 2013

Correspondence to: K. Nishina (kazuya.nishina@gmail.com)

Published by Copernicus Publications on behalf of the European Geosciences Union.

Abstract

Soil organic carbon (SOC) is the largest carbon pool in terrestrial ecosystems and may play a key role in biospheric feedback to elevated atmospheric carbon dioxide (CO_2) in the warmer future world. We examined seven biome models with climate projections forced by four representative-concentration-pathways (RCPs)-based atmospheric concentration scenarios. The goal was to specify uncertainty in global SOC stock projections from global and regional perspectives. Our simulations showed that SOC stocks among the biome models varied from 1090 to 2650 Pg C even in historical periods (ca. 2000). In a higher forcing scenario (RCP8.5), inconsistent estimates of impact on the total SOC (2099–2000) were obtained from different model simulations, ranging from a net sink of 347 Pg C to a net source of 122 Pg C. In all models, the elevated atmospheric CO_2 concentration in the RCP8.5 scenario considerably contributed to carbon accumulation in SOC. However, magnitudes varied from 93 to 264 Pg C by the end of the 21st century. Using time-series data of total global SOC estimated by biome biome model, we statistically analyzed the sensitivity of the global SOC stock to global mean temperature and global precipitation anomalies (ΔT and ΔP respectively) in each biome model using a state-space model. This analysis suggests that ΔT explained global SOC stock changes in most models with a resolution of 1–2 °C, and the magnitude of global SOC decomposition from a 2 °C rise ranged from almost 0 Pg C yr^{-1} to 3.53 Pg C yr^{-1} among the biome models. On the other hand, ΔP had a negligible impact on change in the global SOC changes. Spatial heterogeneity was evident and inconsistent among the changes in SOC estimated by the biome models, especially in boreal to arctic regions. Our study revealed considerable climate change impact uncertainty in SOC decomposition among biome models. Further research is required to improve our understanding and ability to estimate biospheric feedback through SOC-relevant processes as well as vegetation processes.

1 Introduction

Although soils form only a thin skin-like covering on the earth's surface, soil organic carbon (SOC) is considered to be the largest carbon pool in terrestrial ecosystems (Davidson and Janssens, 2006). Soil provides many ecosystem services, such as regulating and provisioning services and societal services (Breure et al., 2012). In ecosystem services, SOC is critical for ensuring sustainable food production owing to its nutrient retention function and water-holding capacity (Lal, 2004, 2010). Thus, the maintenance of SOC is important for global and social sustainability (e.g. Mol and Keesstra, 2012). In climate systems, because of the vast carbon pool of SOC, the behavior of SOC is key for understanding the feedback of terrestrial ecosystems to atmospheric CO_2 concentrations in a warmer world (Heimann and Reichstein, 2008; Thum et al., 2011). However, a large number of uncertainties exist in the observation and modeling of SOC dynamics (e.g. Post et al., 1982; Todd-Brown et al., 2013). For example, in the Coupled Model Intercomparison Project Phase 5 (CMIP5), Todd-Brown et al. (2013) reported that the present-day global SOC stocks range from 514 to 3046 Pg C among 11 Earth system models (ESMs). Soil processes in terrestrial ecosystem models are significantly simpler than actual processes or above-ground processes, and thus exacerbate uncertainties in future projections of SOC dynamics.

Temperature and precipitation are critical factors for the feedback of terrestrial ecosystems to atmospheric CO_2 (Seneviratne et al., 2006). Similarly, SOC dynamics are strongly affected by temperature and precipitation, because SOC dynamics in biome models are parameterized as a function of soil temperature, moisture, and other factors (e.g. Davidson and Janssens, 2006; Ise and Moorcroft, 2006; Falloon et al., 2011). The differences in these functions and their parameters have important effects on the projection of global SOC stocks (Davidson and Janssens, 2006; Ise and Moorcroft, 2006).

In this study, we examined the SOC dynamics in seven biome models obtained from the Inter-Sectoral Impact Model Intercomparison Project (ISI-MIP) (Warszawski et al.,

2013), which were simulated using five global climate models (GCMs) in newly developed climate scenarios, i.e., representative concentration pathways (RCPs). We aimed to explore the uncertainties in future global SOC stock projections and investigate the impact of climate change on the global SOC stock with respect to changes in global mean temperature and precipitation.

We focused on the interannual global SOC dynamics in the biome models under the assumption that SOC is a one-compartment of Earth system. First, we considered global SOC dynamics as the following simple differential equation:

$$\frac{\mathrm{dSOC}}{\mathrm{d}t} = \mathrm{Input} - k\mathrm{SOC} \quad (1)$$

where Input is carbon derived primarily from photosynthesis products via chemical and microbial humification (Wershaw, 1993), and k is the global SOC turnover rate. In most models, SOC decomposition functions as a first-order kinetics process. Thus, SOC dynamics are regulated by the balance between the input from vegetation biomass carbon and SOC decomposition. In this study, we examined a simple hypothesis: can global mean temperature and precipitation anomalies (ΔT (°C) and ΔP (%), respectively) be used as indexes of global SOC decomposition dynamics in future projections? If true, this would mean that ΔT and ΔP can explain the global SOC turnover rate k during a projection period in biome models. This simplification enables us to review the global impact of climate change on SOC. Subsequently, we assessed whether the time evolution of the estimation uncertainties for SOC can be explained by ΔT and ΔP sensitivities during the 21st century for each biome model. Furthermore, we compared the spatial distributions of global SOC pools and their changes to evaluate regional differences, focusing on detailed processes in the interaction with vegetation dynamics.

2 Materials and methods

2.1 Method and models

In this study, we examined SOC processes using seven biome models obtained from the ISI-MIP. The biome models are Hybrid (Friend and White, 2000), JeDi (Pavlick et al., 2012), JULES (Clark et al., 2011), LPJmL (Sitch et al., 2003), SDGVM (Woodward et al., 1995), VISIT (Ito and Oikawa, 2002; Ito and Inatomi, 2012), and ORCHIDEE (Krinner et al., 2005). In this study, Hybrid, Jedi, LPJmL, and ORCHIDEE are dynamic global vegetation models, and the others are fixed vegetation models, in this study. General information about SOC processes is summarized in Table 1.

These models are simulated in 5 GCM × 4 RCP scenarios and a fixed CO_2 control with RCP8.5 climate condition scenarios. For the biome model forcing, we used climate variables in HadGEM2-ES (HadGEM) with bias correction for temperature and precipitation from Hempel et al. (2013). The global climate variables (atmospheric CO_2 concentration, global mean terrestrial temperature anomaly ΔT (°C), and global terrestrial precipitation anomaly ΔP (%)) in each RCP scenario for HadGEM are summarized in Fig. 1. ΔT and ΔP were set to 0 as the averages of their values between 1980 and 2000. In addition, there was no anthropogenic land-use change for the entire simulation period in this study. More detail about the experimental setup is available in the literature Warszawski et al. (2013).

2.2 Estimation of ΔT and ΔP sensitivity of global SOC

We used a state-space model (more properly vector autoregression) (Sims and Zha, 1998) to evaluate the sensitivity of global SOC decomposition to global temperature and precipitation anomalies in each biome model. This vector autoregression model considers only process uncertainty, not observation uncertainty in a state-space model. We applied this analysis to annual global SOC time-series data in each biome model

simulated in the five scenarios (except for ORCHIDEE), i.e. the four RCPs and the fixed CO_2 experiment with RCP8.5 climate conditions in HadGEM (Figs. 1 and 2).

We first modeled the likelihood function using the following equation. The model outputs are calculated for each year; therefore, we discretized the equation as the annual time step t.

$$\mathrm{SOC}_{[n,t]} \sim \mathrm{normal}(\mu_{[n,t-1]}, \sigma_{\mathrm{ps}}) \tag{2}$$

where $\mathrm{SOC}_{[n,t]}$ is the global SOC stock at time t (year) in scenario n, and σ_{ps} is the process error. $\mu_{[n,t-1]}$ is defined as follows:

$$\mu_{[n,t-1]} = \alpha \mathrm{VegC}_{[n,t-1]} + e^{(-k-\beta_1 \Delta T_{[n,t-1]} - \beta_2 \Delta P_{[n,t-1]})} \mathrm{SOC}_{[n,t-1]} \tag{3}$$

where $\mathrm{VegC}_{[n,t]}$ indicates the global vegetation biomass C stock at time t in scenario n, and α is the fraction of VegC transformed into SOC per year, which is assumed to represent the annual input of SOC. k is the turnover rate for global SOC (yr^{-1}) under standardized global mean temperature and precipitation conditions (averages between 1980 and 2000). β_1 and β_2 are the global SOC sensitivities to ΔT and ΔP, respectively (units: $\mathrm{yr}^{-1}\,\Delta T^{-1}$ and $\mathrm{yr}^{-1}\,\Delta P^{-1}$).

The priors of these parameters are defined as follows:

$$\sigma_{\mathrm{ps}} \sim \mathrm{uniform}\ (0, 100) \tag{4}$$
$$\alpha \sim \mathrm{uniform}\ (0, 0.1) \tag{5}$$
$$k \sim \mathrm{uniform}\ (0, 1) \tag{6}$$
$$\beta_1 \sim \mathrm{normal}\ (0, 100) \tag{7}$$
$$\beta_2 \sim \mathrm{normal}\ (0, 100) \tag{8}$$

We used vague priors for β_1 and β_2 to estimate the ΔT and ΔP effect on the global SOC turnover rate k. For α and k, we used uniform priors, which are sufficiently broad theoretically.

Then, the joint posterior is given by following equation.

$$p(\alpha, \beta_1, \beta_2, k, \sigma_{\mathrm{pr}}|\mathrm{data}) \sim p(\mathrm{data}|\alpha, \beta_1, \beta_2, k, \sigma_{\mathrm{pr}}) \times p(\alpha)p(k)p(\beta_1)p(\beta_2)p(\sigma_{\mathrm{pr}}) \tag{9}$$

We used the Hamiltonian Monte Carlo method to sample the posterior with STAN (Stan Development Team, 2012) and R (R Core Team, 2012).

3 Results

3.1 Global SOC and VegC projection in HadGEM

The increase of ΔT depends on the RCP scenario, with the maximum increase in RCP8.5 being 5.2 °C in 2099. In RCP2.6, the maximum ΔT was 1.9 °C during the entire simulation period and showed signs of leveling off in 2050. In all RCP scenarios, ΔP increased: to 11 % (RCP4.5) and to 16 % (RCP8.5). However, there were high amplitudes of ΔP in each RCP scenario; thus, there were no obvious differences between RCPs.

For 2000 in HadGEM, the global SOC stocks varied from 1090 Pg C (Hybrid) to 2646 Pg C (LPJmL) in the biome models (Fig. 2). The mean global SOC stock in the six models was 1772 Pg C (standard deviation; 568 Pg C). The estimated empirical global SOC stock was 1255 Pg C (Todd-Brown et al., 2013). On the other hand, global VegC stocks in 2000 ranged from 510 Pg C (VISIT) to 1023 Pg C (JULE). The mean global VegC among the seven biome models was 809 Pg C (S.D.; 223 Pg C) (Fig. 2). The global VegC stocks in most models were comparable with the VegC (493 Pg C) estimated by the IPCC Tier-1 method (Ruesch and Gibbs, 2008).

In the projection period (2000–2099), the SOC stock in the six models (except for Hybrid) increased in all RCPs compared to that in 2000. The global SOC stock in Hybrid continuously decreased in all RCPs during the projection period (Fig. 2). Under the RCPs, the maximum SOC stock increase for the projection period was observed

in JeDi with RCP8.5, with a value of 347 Pg C. In the fixed CO_2 scenarios, the global SOC stocks continuously decreased in most biome models (except in Hybrid), showing global SOC changes from −299 to 65 Pg C at the end of the simulation period.

The global VegC stocks increased in nearly all RCPs and biome models compared to the global VegC in 2000. However, the global VegC stocks in Hybrid and LPJmL with RCP8.5 did not continuously increase in the projection period and were not the largest stock at the end of the simulation period. In the fixed CO_2 scenarios, the global VegC stocks also continuously decreased, and global VegC changes ranged from −527 to −40 Pg C at the end of the simulation period (Fig. 2).

The order of the SOC stock in each RCP at the end of the simulation (2099) is in good agreement with the order of each corresponding VegC stock in the same period in JeDi, JULES, LPJmL, and SDGVM. However, the orders of the SOC stock in the other biome models are different than those of the global VegC stocks. These stock changes are attributed to the different SOC decomposition processes.

3.2 Posteriors of the state-space model; global SOC sensitivity to ΔT and ΔP

The Gelman and Rubin convergence statistics ($\hat{R}$) of all parameters were lower than 1.01 in all models; therefore, the parameters represented successful convergences (data not shown). The posterior distributions of the parameters for each biome model are summarized in Table 1.

α, which is the fraction of annual translation of VegC to SOC, among the biome models varied from 0.721 % in Hybrid to 3.860 % in VISIT. The SOC turnover rate $k\,\mathrm{yr}^{-1}$ ranged from $2.51 \times 10^{3}\,\mathrm{yr}^{-1}$ in LPJmL to $16.10 \times 10^{3}\,\mathrm{yr}^{-1}$ in VISIT.

The 95 % credible intervals (CI) in sensitivity of global SOC to ΔT (β_1) in each biome model did not cover 0 in all models (Table 2). And the 95 % CI of β_1 in each model were not partially duplicated, which means that the sensitivity to ΔT could be statistically distinguished between the biome models. The highest β_1 was observed in VISIT, with

a median value of $1.225 \times 10^{-3}\,\mathrm{yr}^{-1}\ \Delta T^{-1}$ (or $^{\circ}\mathrm{C}^{-1}$). The lowest β_1 was observed in JeDi and was approximately $0\,\mathrm{yr}^{-1}\ \Delta T^{-1}$.

The sensitivity of global SOC to ΔP (β_2) in the biome models was lower compared to the SOC turnover rate k and β_1. Their values ($\mathrm{yr}^{-1}\,\Delta P^{-1}$) were nearly one order of magnitude less than β_1. Considering the range of the values of ΔP in the projection period, the impact on global SOC stock dynamics is small in all biome models. Furthermore, the 95 % CIs of β_2 in each model were partially duplicated.

On the basis of the posterior parameters, we estimated the stimulated global SOC decomposition for Δ2 °C, Δ3 °C, and Δ4 °C, assuming that each global SOC stock is at the 2000 level (Fig. 3). A statistical difference was observed among the Δ2 °C, Δ3 °C, and Δ4 °C in five biome models (i.e. Hybrid, JULES, LPJmL, VISIT, and ORCHIDEE). However, the magnitudes of the stimulated global SOC decomposition varied. At Δ4 °C, it ranged from 1.9 Pg C yr^{-1} (in LPJmL) to 8.1 Pg C yr^{-1} (in JULES). In SDGVM, there were no statistical differences in the stimulated global SOC decomposition between Δ3 °C and Δ4 °C. There were also no differences in this term among Δ2 °C, Δ3 °C, and Δ4 °C in JeDi.

3.3 Latitudinal δSOC (2099–2000 and CO_2–Fixed CO_2) in HadGEM RCP8.5

In all biome models, large SOC stocks were observed in high-latitude zones (50° N to 75° N; Figs. 5a and Supplement Fig. S1). However, the range of SOC accumulation (kg-C m^{-2}) in each biome model was different. The upper 99th percentile of SOC accumulation in each biome model varied from 23.8 kg-C m^{-2} in SDGVM to 97.6 kg-C m^{-2} in LPJmL (Fig. S1).

For differences between 2099 and 2000 in HadGEM RCP8.5, a large variance among biome models was observed between 30° S and 10° N (Tropic region) and between 40° N and 75° N (Boreal to Arctic region) (Figs. 4 and 5a) in the biome models. There were four types of latitudinal changes: (i) SOC increase in both regions (JeDi, SDGVM, ORCHIDEE); (ii) SOC increase in boreal to arctic regions and decrease in

the tropics (JULES, VISIT); (iii) SOC increase in the tropics and decrease in boreal to arctic regions (LPJmL); and (iv) SOC decrease in both regions (Hybrid). The maximum difference was observed in the boreal regions, where it reached more than 20 Pg $2.5^{\circ -1}$.

There were also differences between the increasing CO_2 scenario to the fixed CO_2 scenario in HadGEM RCP8.5 (Fig. 5c). This suggests an indirect CO_2 fertilizer effect on the SOC stocks due to plant production and biomass increases because of the increase in photosynthesis under high CO_2 concentration. We observed bimodal increases in six biome models, and the peaks were between 30° N and 70° N and between 30° S and 10° N. In Hybrid, the large SOC increase due to CO_2 was unimodal around the boreal regions. The maximum difference between the increasing CO_2 scenario and the fixed CO_2 scenario was observed around 60° N, which was approximately 10 Pg $2.5^{\circ -1}$

4 Discussion

4.1 Global mean temperature and precipitation impact on global SOC decomposition and projection uncertainties

During the projection period (2000–2099), the global SOC stock changes in all RCPs (without the fixed CO_2 scenario) ranged from −6 Pg C to 280 Pg C under RCP2.6 (mean ± S.D.: 89 ± 104 Pg C). Under RCP8.5, the SOC changes varied from −124 Pg C to 392 Pg C (113 ± 176 Pg C) (Fig. 2) at the end of the projection period. This global SOC stock changes are equivalent to −58 to +185 ppmv in atmospheric CO_2 concentration. Thus, in higher radiative forcing scenarios, uncertainties associated with future global SOC projection increase. These ranges of the global SOC stock changes by 2099 were comparable with the VegC changes (Fig. 2). However, in the projection period, the global VegC stocks primarily act as sinks for atmospheric CO_2, while the global SOC stocks act as both sinks and sources depending on the biome model. There were consistent SOC projections in the same period (2000–2100) from multiple model simulations in previous studies. In a C4MIP study, the global SOC stock changes ranged

from approximately −50 to 300 Pg by the end of the simulation period among the 11 coupled carbon models (Friedlingstein et al., 2006; Eglin et al., 2010). It has also been reported that SOC stocks in 2100 differ by approximately 200 Pg among five DGVMs under forced A1FI and B1 scenarios Sitch et al. (2008), which is the highest forcing scenario in AR4 assessment. Compared with these studies, the SOC changes simulated in this study varied comparably or showed slightly higher uncertainty than those of previous projections.

To put it simply, the magnitude of global SOC decomposition and the response to ΔT primarily depend on the amount of the global SOC stock due to a first-order kinetic SOC decomposition process. As has been reported in a CMIP5 experiment (Todd-Brown et al., 2013), our study has also shown that simulated global present-day SOC stocks in seven ecosystem models show high variation (1090–2646 Pg C) compared to the variation of global present-day VegC stocks (Fig. 2). This SOC stock uncertainty invokes future projection uncertainty in SOC dynamics. To test this issue, we estimated the global SOC standardized impact of each ΔT by a simple substitution, which assumed that the global SOC stock in each biome model is equal to the value (1255 Pg C, 95 % C.I.; 891–1657 Pg C) reported in a previous study (Todd-Brown et al., 2013). The standardized global SOC decomposition was smaller than the original SOC decomposition in some models, which showed large differences in the global SOC stocks compared to the reference SOC stock (Todd-Brown et al., 2013) (Figs. 2 and 5). In addition, overall uncertainties among the biome models became relatively small. This also indicates that global SOC estimation is critical to the magnitude of SOC feedback. Thus, the estimated dynamic model revealed that the sensitivity of global SOC to ΔT varied among the biome models and that the present-day global SOC stock can be used to make more reliable SOC projections. Although global SOC stock estimation still has significant uncertainty, global SOC stock constraints are essential for reducing uncertainty in global SOC projections in ecosystem models.

Our simplified global dynamic model for the global SOC stock revealed that the balance of the global SOC stock turnover and input from VegC is quite different among

the biome models, which further implies the different sensitivities to ΔT of the global SOC stocks among the biome models (Table 1). Hybrid simulated global SOC stocks decrease by 2099 in all RCPs because of the relatively high ΔT sensitivity in addition to the low turnover rate (high residence time) in VegC to SOC (Table 2, (Friend et al., 2013)). Although temperature is the most significant regulation factor of SOC dynamics (Raich and Schlesinger, 1992), discussion of the effect of increasing global mean temperature on SOC stocks is still lacking. According to our statistical analysis (Table 2), most biome models had adequate resolution to describe the global SOC stock change among the Δ 1 °C (or 2 °C for SDGVM) difference in the projection period. In these models, the global mean temperature ΔT could be a measure of the robustness of global SOC stock projection. On the other hand, the global SOC in JeDi was not sensitive to ΔT in this projection period. According to our estimation, the highest global SOC sensitivity was observed in VISIT, in which the rate of global SOC stock change was enhanced by $-6.95\,\mathrm{Pg\,C\,yr^{-1}}$ in $\Delta 4\,^{\circ}\mathrm{C}$ (Fig. 3). However, the highest magnitude of SOC decomposition stimulated by increasing ΔT was observed in JULES ($-8.13\,\mathrm{Pg\,C\,yr^{-1}}$ in $\Delta 4\,^{\circ}\mathrm{C}$) due to high global SOC stock in JULES. This value might not be extremely high. The Carnegie-Ames-Stanford approach model showed global SOC decomposition sensitivity of $2.26\,\mathrm{Pg\,C\,yr^{-1}\Delta\,^{\circ}C^{-1}}$ in this model, which is nearly equivalent to results obtained from JULES when the $\Delta 4\,^{\circ}\mathrm{C}$ value was derived from simple extrapolation (Zhou et al., 2009). On the other hand, Raich et al. (2002) and Zhou et al. (2009) reported global soil respiration sensitivity (including root respiration and SOC decomposition), estimated by an empirical model with a global soil respiration dataset, of $3.3\,\mathrm{Pg\,C\,yr^{-1}\Delta\,^{\circ}C^{-1}}$ and $3.21\,\mathrm{Pg\,C\,yr^{-1}\Delta\,^{\circ}C^{-1}}$, respectively. Although these values are not directly comparable to SOC decomposition responsiveness, but to SOC decomposition response in the almost biome models in this study, their sensitivity could be underestimated. There is still a lack of observation-based estimation of global SOC response intensity to ΔT. Both global SOC stocks and a data-oriented parameter such as this may be important information for the constraint and validation of global SOC dynamics.

On the other hand, β_2 was not effective for global SOC dynamics in all ecosystem models in our analysis. This does not mean that precipitation is not important in SOC dynamics. Precipitation trends are globally heterogeneous; therefore, the representative ΔP might not be a useful index of SOC stock dynamics at a global scale in this projection period. However, precipitation is quite important in both soil decomposition (Falloon et al., 2011) and vegetation processes (Seneviratne et al., 2006), which considerably contribute to regional SOC dynamics.

4.2 SOC stock changes from vegetation dynamics and regional aspect

There were consistent latitudinal (geographic) patterns among the biome models (Figs. 5a and Fig. 1), and the highest SOC stock was observed between 40° N and 75° N. However, we found that the amount of SOC stocks among the biome models significantly vary in this region. The model SOC densities are different, possibly because of the balance of input and decomposition and the consideration of depth in the biome models (1 to 3 m or not explicit, Table 1). Tarnocai et al. (2009) estimated SOC stock depth up to 3 m, with a value of 1672 Pg C in permafrost-affected regions only. Thus, the SOC stock of this region and the global SOC stock in the biome models may be significantly underestimated.

From a regional perspective of SOC projection, the biome models showed quite different spatial patterns of SOC changes in HadGEM RCP8.5 (Figs. 4 and 5), while the spatial patterns of VegC changes were generally consistent among the biome models (Friend et al., 2013). We found that this spatial heterogeneity among the biome models was also present in the SOC stock changes in different scenarios (data not shown). In particular, in boreal to arctic regions, SOC acts as a sink and source of C depending on the biome model (Fig. 5). This result indicates that there is an underlying mechanistic difference among the biome models in these regions. Two models show decreased SOC stocks by 2099 in this region in HadGEM RCP8.5. LPJmL, which is a freeze-and-thaw thermodynamics explicit DGVM model, shows outstanding features in SOC stocks and changes in this region. This implies that high SOC accumulations

(over 80 kg-C m^{-2}) (Figs. 5 and Fig. S1) will be reduced with decreasing VegC by 2099 (Fig. S2) in this region. This trend would result in low water availability in the permafrost regions, because the prediction is based on a mechanistic freeze–thaw scheme (Beer et al., 2007). On the other hand, in Hybrid, SOC decomposition is the main factor contributing to reduced SOC in this region. Dynamic vegetation and freeze–thaw schemes are important for SOC dynamics in permafrost zones, because they provide more accurate prediction of the balance of C input from successive vegetation and old soil carbon decomposition (Schuur et al., 2008, 2009; Schaphoff et al., 2013). However, in this study, dynamic vegetation and freeze–thaw schemes are only implemented in LPJmL. The potential release from SOC in permafrost regions could have a large impact on the global C cycle (Koven et al., 2011; Burke et al., 2012; MacDougall et al., 2012), and further model development is essential for the modification of projections for this region.

Previous extensive field research has shown that the CO_2 fertilizer effect on plant growth in higher CO_2 concentrations could also result in the accumulation of SOC in regional ecosystems (De Graaff et al., 2006). In the RCP 8.5 climate condition, the fixed CO_2 experiment suggested that the CO_2 fertilizer effect on plant production considerably contributed to the global SOC stock increase in all biome models. The indirect CO_2 fertilizer effect on the global SOC stock varied from 93 Pg C (Hybrid) to 264 Pg C (VISIT) (mean ± S.D.; 196 ± 60 Pg C) at the end of the simulation period, while VegC stock increased from 295 to 645 Pg C (275 ± 150 Pg C) by 2099 because of increasing CO_2 (Figs. 2 and S2). Thus, the CO_2 fertilizer effect on global SOC accumulation strongly affects the biome models, and further quantitative assessment might be needed. For example, Friend et al. (2013) focused their attention on the effects of CO_2 fertilizers on biomass production.

4.3 SOC modeling issues

The accurate estimation of present-day global SOC stock remains difficult because of a lack of appropriate broad and non-destructive investigation techniques to measure SOC stock, such as satellite-based remote sensing. In addition, global long-term SOC stock dynamics for model validation are limited. Thus, it is difficult to assess projected global SOC trends in each biome model. Therefore, in addition to quantitatively understanding the SOC stock, deductive inferences based on the extensive understanding of the processes are essential for minimizing uncertainties in SOC stock prediction. For example, the apparent variability in global SOC sensitivity to ΔT may result from differences in model structures and parameters. Regarding temperature sensitivity and the magnitude of response to rising temperatures, the following topics require improvement: (i) SOC compartments and their turnover rates (Jones et al., 2005; Conant et al., 2011); (ii) the temperature sensitivity parameter (e.g. Q_{10}) (Davidson and Janssens, 2006; Allison et al., 2010); and (iii) soil temperature prediction (radiation, heat production by microbes) (Luke and Cox, 2011; Khvorostyanov et al., 2008). In addition, microbial dynamics is a key component for the temperature acclimation of SOC decomposition (Todd-Brown et al., 2012; Wang et al., 2013). The acclimation response of SOC decomposition by microbial physiology is not included in the biome models used in this study. For SOC accumulation, soil mineralogical properties control soil C turnover (Torn et al., 1997). However, the biome models do not exploit global soil classification information (i.e. volcanic or non-volcanic soils), which still has significant uncertainties (Guillod et al., 2012; Hiederer and Köchy, 2011). In this study, peat and wetland soils are not explicitly simulated because of the large simulation grid size. Because of large carbon stock and water regime changes in future climates in such ecosystems, SOC and soil-water-holding capacity feedback should also be considered in the SOC process in biome models (Ise et al., 2008).

However, the details of these processes are beyond the scope of this study; therefore, we did not explore these issues in depth. A more specific model intercomparison,

such as an environmental-response-function-based assessment (e.g. Falloon et al., 2011; Sierra et al., 2012) should be effective. Furthermore, Land-use change is not included in our projection; however, the effect of land-use changes on SOC dynamics is critical (Eglin et al., 2010). Estimating land-use change with high confidence is essential for accurate global SOC stock projections and could be used as a basis for policies that moderate the impacts of climate change.

5 Conclusions

The uncertainties associated with SOC projections are significantly high. The projected global SOC stocks by 2099 act as CO_2 sources and sinks depending on the biome models, even though models have captured historical SOC trends reasonably. The uncertainties of the SOC changes increase with higher forcing scenarios, and the global SOC stock changes vary from −157 to 225 Pg C in HadGEM RCP8.5.

By adopting the simplified approach of global SOC as one compartment in the Earth system, we can understand the comprehensive characteristics of each biome model on a global scale. The magnitude of SOC feedback and resolution of the increase in global mean temperature considerably differed depending on the biome model. Our results confirmed that the SOC processes are dissimilar among the biome models on a global scale. In addition, global precipitation anomalies could not explain the future global SOC stock changes. Moreover, the indirect CO_2 fertilizer effect immensely contributed to global SOC stock changes and projection uncertainties. For more reliable projections, both SOC dynamics and vegetation processes may require reliable global SOC stock estimation and region-based improvements.

Supplementary material related to this article is available online at http://www.earth-syst-dynam-discuss.net/4/1035/2013/esdd-4-1035-2013-supplement.pdf.

Acknowledgements. The authors wish to thank the ISI-MIP coordination team from the Potsdam Institute for Climate Impact Research. We acknowledge the World Climate Research Programme's Working Group on Coupled Modelling, which is responsible for CMIP. We also thank the climate modeling groups for producing and making their model output available. This study has been conducted under the ISI-MIP framework. The ISI-MIP Fast Track project was funded by the German Federal Ministry of Education and Research, project funding reference number 01LS1201A. Responsibility for the content of this publication lies with the authors. We also thank Naota Hanasaki and Yoshimitsu Masaki from the NIES for supporting the preparation of ISI-MIP settings. We appreciate the valuable comments from Seita Emori (NIES), Yoshiki Yamagata (NIES), and Rota Wagai (NIAES). This study was supported in part by the Environment Research and Technology Development Fund (S-10) of the Ministry of the Environment, Japan.

References

Allison, S. D., Wallenstein, M. D., and Bradford, M. A.: Soil-carbon response to warming dependent on microbial physiology, Nat. Geosci., 3, 336–340, 2010. 1050

Beer, C., Lucht, W., Gerten, D., Thonicke, K., and Schmullius, C.: Effects of soil freezing and thawing on vegetation carbon density in Siberia: A modeling analysis with the Lund-Potsdam-Jena Dynamic Global Vegetation Model (LPJ-DGVM), Global Biogeochem. Cy., 21, GB1012, doi:10.1029/2006GB002760, 2007. 1049

Breure, A., De Deyn, G., Dominati, E., Eglin, T., Hedlund, K., Van Orshoven, J., and Posthuma, L.: Ecosystem services: a useful concept for soil policy making!, Curr. Opin. Environ. Sus., 4, 578–585, 2012. 1038

Burke, E. J., Hartley, I. P., and Jones, C. D.: Uncertainties in the global temperature change caused by carbon release from permafrost thawing, The Cryosphere, 6, 1063–1076, doi:10.5194/tc-6-1063-2012, 2012. 1049

Clark, D. B., Mercado, L. M., Sitch, S., Jones, C. D., Gedney, N., Best, M. J., Pryor, M., Rooney, G. G., Essery, R. L. H., Blyth, E., Boucher, O., Harding, R. J., Huntingford, C., and Cox, P. M.: The Joint UK Land Environment Simulator (JULES), model description – Part 2: Carbon fluxes and vegetation dynamics, Geosci. Model Dev., 4, 701–722, doi:10.5194/gmd-4-701-2011, 2011. 1040, 1058

Conant, R., Ryan, M., Ågren, G., Birge, H., Davidson, E., Eliasson, P., Evans, S., Frey, S., Giardina, C., Hopkins, F., Hyvönen, R., Kirschbaum, M. U. F., Lavallee, J. M., Leifeld, J., Parton, W. J., Megan Steinweg, J., Wallenstein, M. D., Martin Wetterstedt, J. Å., and Bradford, M. A.: Temperature and soil organic matter decomposition rates–synthesis of current knowledge and a way forward, Global Change Biol., 17, 3392–3404, doi:10.1111/j.1365-2486.2011.02496.x, 2011. 1050

Davidson, E. and Janssens, I.: Temperature sensitivity of soil carbon decomposition and feedbacks to climate change, Nature, 440, 165–173, 2006. 1038, 1050

De Graaff, M. A., Van Groningen, K. J. A. N., Six, J., Hungate, B., and van Kessel, C.: Interactions between plant growth and soil nutrient cycling under elevated CO_2: A meta-analysis, Global Change Biol., 12, 2077–2091, 2006. 1049

Eglin, T., Ciais, P., Piao, S., Barre, P., Bellassen, V., Cadule, P., Chenu, C., Gasser, T., Koven, C., Reichstein, M., and Smith, P.: Historical and future perspectives of global soil carbon response to climate and land-use changes, Tellus B, 62, 700–718, 2010. 1046, 1051

Falloon, P., Jones, C., Ades, M., and Paul, K.: Direct soil moisture controls of future global soil carbon changes: An important source of uncertainty, Global Biogeochem. Cy., 25, GB3010, doi:10.1029/2010GB003938, 2011. 1038, 1048, 1051

Friedlingstein, P., Cox, P., Betts, R., Bopp, L., Von Bloh, W., Brovkin, V., Cadule, P., Doney, S., Eby, M., Fung, I., Bala, G., John, J., Jones, C., Joos, F., Kato, T., Kawamiya, M., Knorr, W., Lindsay, K., Matthews, H. D., Raddatz, T., Rayner, P., Reick, C., Roeckner, E., Schnitzler, K. G., Schnur, R., Strassmann, K., Weaver, A. J., Yoshikawa, C., and Zeng, N.: Climate-carbon cycle feedback analysis: Results from the C4MIP model intercomparison, J. Climate, 19, 3337–3353, 2006. 1046

Friend, A. D. and White, A.: Evaluation and analysis of a dynamic terrestrial ecosystem model under preindustrial conditions at the global scale, Global Biogeochem. Cy., 14, 1173–1190, 2000. 1040, 1058

Friend, A. D., Betts, R., Cadule, P., Ciais, P., Clerk, D., Dankers, R., Falloon, P., Gerten, D., Itoh, A., Kahana, R., Keribin, R. M., Kleidon, A., Lomas, M. R., Nishina, K., Ostberg, S., Pavlick, R., Peylin, P., Rademacher, T. T., Schaphoff, S., Vuichard, N., Wiltshire, A., and Woodward, F. I.: Anticipating terrestrial ecosystem response to future climate change and increase in atmospheric CO_2, Proc. Natl. Acad. Sci. USA, in press, 2013. 1047, 1048, 1049

Guillod, B., Davin, E., Kündig, C., Smiatek, G., and Seneviratne, S.: Impact of soil map specifications for European climate simulations, Clim. Dynam., 40, 1–19, 2012. 1050

Heimann, M. and Reichstein, M.: Terrestrial ecosystem carbon dynamics and climate feedbacks, Nature, 451, 289–292, 2008. 1038

Hempel, S., Frieler, K., Warszawski, L., Schewe, J., and Piontek, F.: A trend-preserving bias correction-the ISI-MIP approach, Earth Syst. Dynam., 4, 219–236, doi:10.5194/esd-4-219-2013, 2013. 1040

Hiederer, R. and Köchy, M.: Global soil organic carbon estimates and the harmonized world soil database, EUR 25225EN, Luxembourg, 2011. 1050

Ise, T. and Moorcroft, P.: The global-scale temperature and moisture dependencies of soil organic carbon decomposition: an analysis using a mechanistic decomposition model, Biogeochem., 80, 217–231, 2006. 1038

Ise, T., Dunn, A., Wofsy, S., and Moorcroft, P.: High sensitivity of peat decomposition to climate change through water-table feedback, Nat. Geosci., 1, 763–766, 2008. 1050

Ito, A. and Inatomi, M.: Water-use efficiency of the terrestrial biosphere: a model analysis focusing on interactions between the global carbon and water cycles, J. Hydrometeorol., 13, 681–694, 2012. 1040, 1058

Ito, A. and Oikawa, T.: A simulation model of the carbon cycle in land ecosystems (Sim-CYCLE): a description based on dry-matter production theory and plot-scale validation, Ecol. Model., 151, 143–176, 2002. 1040

Jones, C., McConnell, C., Coleman, K., Cox, P., Falloon, P., Jenkinson, D., and Powlson, D.: Global climate change and soil carbon stocks; predictions from two contrasting models for the turnover of organic carbon in soil, Global Change Biol., 11, 154–166, 2005. 1050

Khvorostyanov, D., Krinner, G., Ciais, P., Heimann, M., and Zimov, S.: Vulnerability of permafrost carbon to global warming. Part I: model description and role of heat generated by organic matter decomposition, Tellus B, 60, 250–264, 2008. 1050

Koven, C., Ringeval, B., Friedlingstein, P., Ciais, P., Cadule, P., Khvorostyanov, D., Krinner, G., and Tarnocai, C.: Permafrost carbon-climate feedbacks accelerate global warming, Proc. Natl. Acad. Sci. USA, 108, 14769–14774, 2011. 1049

Krinner, G., Viovy, N., de Noblet-Ducoudré, N., Ogée, J., Polcher, J., Friedlingstein, P., Ciais, P., Sitch, S., and Prentice, I.: A dynamic global vegetation model for studies of the coupled atmosphere-biosphere system, Global Biogeochem. Cy., 19, GB1015, doi:10.1029/2003GB002199, 2005. 1040, 1058

Lal, R.: Soil carbon sequestration impacts on global climate change and food security, Science, 304, 1623–1627, 2004. 1038

Lal, R.: Beyond Copenhagen: mitigating climate change and achieving food security through soil carbon sequestration, Food Secur., 2, 169–177, 2010. 1038
Luke, C. and Cox, P.: Soil carbon and climate change: from the Jenkinson effect to the compost-bomb instability, Eur. J. Soil Sci., 62, 5–12, 2011. 1050
MacDougall, A., Avis, C., and Weaver, A.: Significant contribution to climate warming from the permafrost carbon feedback, Nat. Geosci., 5, 719–721, doi:10.1038/ngeo1573, 2012. 1049
Mol, G. and Keesstra, S.: Soil science in a changing world, Curr. Opin. Environ. Sus., 4, 473–477, doi:10.1016/j.cosust.2012.10.013, 2012. 1038
Pavlick, R., Drewry, D. T., Bohn, K., Reu, B., and Kleidon, A.: The Jena Diversity-Dynamic Global Vegetation Model (JeDi-DGVM): a diverse approach to representing terrestrial biogeography and biogeochemistry based on plant functional trade-offs, Biogeosciences Discuss., 9, 4627–4726, doi:10.5194/bgd-9-4627-2012, 2012. 1040, 1058
Post, W., Emanuel, W., Zinke, P., and Stangenberger, A.: Soil carbon pools and world life zones, Nature, 298, 156–159, 1982. 1038
R Core Team: R: A Language and Environment for Statistical Computing, R Foundation for Statistical Computing, Vienna, Austria, available at: http://www.R-project.org/, ISBN 3-900051-07-0, 2012. 1042
Raich, J. and Schlesinger, W.: The global carbon dioxide flux in soil respiration and its relationship to vegetation and climate, Tellus B, 44, 81–99, 1992. 1047
Raich, J. W., Potter, C. S., and Bhagawati, D.: Interannual variability in global soil respiration, 1980–94, Global Change Biol., 8, 800–812, 2002. 1047
Ruesch, A. and Gibbs, H. K.: New IPCC Tier-1 global biomass carbon map for the year 2000, Carbon Dioxide Information Analysis Center (CDIAC), Oak Ridge National Laboratory, Oak Ridge, Tennessee, available at: http://cdiac.ornl.gov (last access: January 2013), 2008. 1042, 1061
Schaphoff, S., Heyder, U., Ostberg, S., Gerten, D., Heinke, J., and Lucht, W.: Contribution of permafrost soils to the global carbon budget, Environ. Res. Lett., 8, 014026, doi:10.1088/1748-9326/8/1/014026, 2013. 1049
Schuur, E., Bockheim, J., Canadell, J., Euskirchen, E., Field, C., Goryachkin, S., Hagemann, S., Kuhry, P., Lafleur, P., Lee, H., Mazhitova, G., Nelson, F. E., Rinke, A., Romanovsky, V. E., Shiklomanov, N., Tarnocai, C., Venevsky, S., Vogel, J. G., and Zimov, S. A.: Vulnerability of permafrost carbon to climate change: Implications for the global carbon cycle, Bioscience, 58, 701–714, 2008. 1049

Schuur, E., Vogel, J., Crummer, K., Lee, H., Sickman, J., and Osterkamp, T.: The effect of permafrost thaw on old carbon release and net carbon exchange from tundra, Nature, 459, 556–559, 2009. 1049
Seneviratne, S., Lüthi, D., Litschi, M., and Schär, C.: Land–atmosphere coupling and climate change in Europe, Nature, 443, 205–209, 2006. 1038, 1048
Sierra, C. A., Müller, M., and Trumbore, S. E.: Models of soil organic matter decomposition: the SoilR package, version 1.0, Geosci. Model Dev., 5, 1045–1060, doi:10.5194/gmd-5-1045-2012, 2012. 1051
Sims, C. and Zha, T.: Bayesian methods for dynamic multivariate models, Int. Econ. Rev., 39, 949–968, 1998. 1040
Sitch, S., Smith, B., Prentice, I., Arneth, A., Bondeau, A., Cramer, W., Kaplan, J., Levis, S., Lucht, W., Sykes, M., Thonicke, K., and Venevsky, S.: Evaluation of ecosystem dynamics, plant geography and terrestrial carbon cycling in the LPJ dynamic global vegetation model, Global Change Biol., 9, 161–185, 2003. 1040, 1058
Sitch, S., Huntingford, C., Gedney, N., Levy, P., Lomas, M., Piao, S., Betts, R., Ciais, P., Cox, P., Friedlingstein, P., Jones, C. D., Prentice, I. C., and Woodward, F. I.: Evaluation of the terrestrial carbon cycle, future plant geography and climate-carbon cycle feedbacks using five Dynamic Global Vegetation Models (DGVMs), Global Change Biol., 14, 2015–2039, 2008. 1046
Stan Development Team: Stan: A C++ Library for Probability and Sampling, Version 1.0, available at: http://mc-stan.org/ (last access: January 2013), 2012. 1042
Tarnocai, C., Canadell, J., Schuur, E., Kuhry, P., Mazhitova, G., and Zimov, S.: Soil organic carbon pools in the northern circumpolar permafrost region, Global Biogeochem. Cy., 23, GB2023, doi:10.1029/2008GB003327, 2009. 1048
Thum, T., Räisänen, P., Sevanto, S., Tuomi, M., Reick, C., Vesala, T., Raddatz, T., Aalto, T., Järvinen, H., Altimir, N., Pilegaard, K., Nagy, Z., Rambal, S., and Liski, J.: Soil carbon model alternatives for ECHAM5/JSBACH climate model: Evaluation and impacts on global carbon cycle estimates, J. Geophys. Res., 116, G02028, doi:10.1029/2010JG001612, 2011. 1038
Todd-Brown, K., Hopkins, F., Kivlin, S., Talbot, J., and Allison, S.: A framework for representing microbial decomposition in coupled climate models, Biogeochem., 109, 19–33, 2012. 1050
Todd-Brown, K. E. O., Randerson, J. T., Post, W. M., Hoffman, F. M., Tarnocai, C., Schuur, E. A. G., and Allison, S. D.: Causes of variation in soil carbon simulations from CMIP5

Earth system models and comparison with observations, Biogeosciences, 10, 1717–1736, doi:10.5194/bg-10-1717-2013, 2013. 1038, 1042, 1046, 1061, 1062

Torn, M., Trumbore, S., Chadwick, O., Vitousek, P., and Hendricks, D.: Mineral control of soil organic carbon storage and turnover, Nature, 389, 170–173, 1997. 1050

Wang, G., Post, W., and Mayes, M.: Development of microbial-enzyme-mediated decomposition model parameters through steady-state and dynamic analyses, Ecol. Appl., 23, 255–272, doi:10.1890/12-0681.1, 2013. 1050

Warszawski, L., et al. (2013 in prep), Research design of the intersectoral impact model intercomparison project (isi-mip), Proc. Natl. Acad. Sci. USA, in preparation, 2013. 1038, 1040

Wershaw, R.: Model for humus in soils and sediments, Environ. Sci. Technol., 27, 814–816, 1993. 1039

Woodward, F., Smith, T., and Emanuel, W.: A global land primary productivity and phytogeography model, Global Biogeochem. Cy., 9, 471–490, 1995. 1040, 1058

Zhou, T., Shi, P., Hui, D., and Luo, Y.: Global pattern of temperature sensitivity of soil heterotrophic respiration (Q_{10}) and its implications for carbon-climate feedback, J. Geophys. Res. Biogeosci., 114, G02016, doi:10.1029/2008JG000850, 2009. 1047

Table 1. Description of SOC-relevant processes in each biome model.

Model	f(T)	f(M)	Compartment	Permafrost	Soil depth	Citation
Hybrid	Exponential with optimum	Optimum curve	8	None	Non-explicit	Friend and White (2000)
JeDi	Exponential (Q_{10}; 1.4)	none	1	None	Over 5 m	Pavlick et al. (2012)
JULES	Exponential (Q_{10}; 2.0)	Linear with plateau	4	None	Non-explicit	Clark et al. (2011)
LPJmL	Lloyd & Taylor	Linear	2	Considered	3 m	Sitch et al. (2003)
SDGVM	Optimum curve	Optimum curve	4	None	1 m	Woodward et al. (1995)
VISIT	Lloyd & Taylor	Optimum curve	1	None	1 m	Ito and Inatomi (2012)
ORCHIDEE	Exponential (Q_{10}; 2.0)	Quadratic	3	None	Non-explicit	Krinner et al. (2005)

Table 2. Posteriors of statistical time-series analysis of each biome model.

Models	$\alpha \times 10^{-2}$ [fraction]	$k \times 10^{-3}$ [yr^{-1}]	$\beta_1 \times 10^{-3}$ [$yr^{-1}\ \Delta T^{-1}$]	$\beta_2 \times 10^{-4}$ [$yr^{-1}\ \Delta P^{-1}$]	σ
Hybrid	0.721 (0.663–0.781)	4.78 (4.35–5.23)	1.130 (0.885–1.039)	0.183 (−0.465–0.111)	0.932 (0.882–0.987)
JeDi	1.815 (1.762–1.867)	7.94 (7.86–8.21)	−0.058 (−0.041−−0.076)	0.001 (−0.006–0.008)	0.442 (0.419–0.467)
Jules	3.727 (3.430–4.033)	13.99 (12.81–15.20)	0.669 (0.613–0.723)	0.333 (0.158–0.504)	1.312 (1.242–1.384)
LPJmL	0.730 (0.687–0.771)	2.51 (2.34–2.68)	0.210 (0.190–0.231)	0.025 (−0.049–0.098)	0.522 (0.495–0.552)
SDGVM	1.820 (1.615–2.030)	6.50 (5.71–7.29)	0.333 (0.266–0.398)	0.365 (0.154–0.575)	0.936 (0.887–0.989)
VISIT	3.860 (3.761–3.958)	16.10 (15.68–16.53)	1.225 (1.181–1.257)	−0.121 (−0.119−−0.151)	0.371 (0.352–0.378)
ORCHIDEE*	1.343 (1.230–1.457)	7.01 (6.38–7.64)	0.903 (0.839–0.970)	−0.009 (−0.031–0.014)	1.001 (0.934–1.076)

* In ORCHIDEE, the parameters were estimated from time-series data compiled three scenarios (RCP2.6, RCP8.5, and Fixed CO_2).

1059

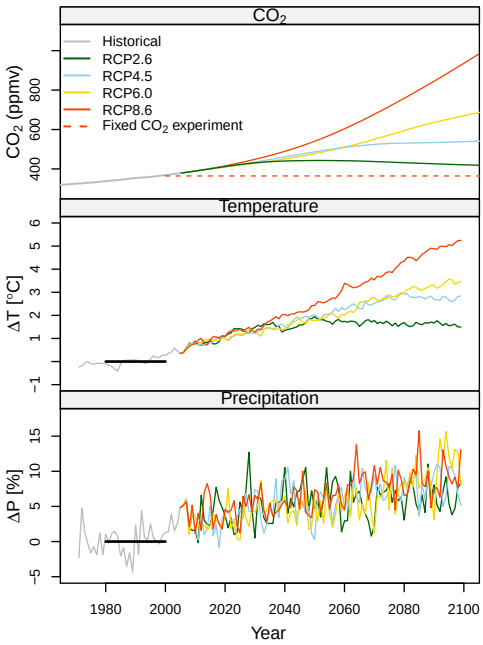

Fig. 1. Climate variables for CO_2 (RCPs), and global mean temperature and global mean precipitation anomalies in HadGEM.

1060

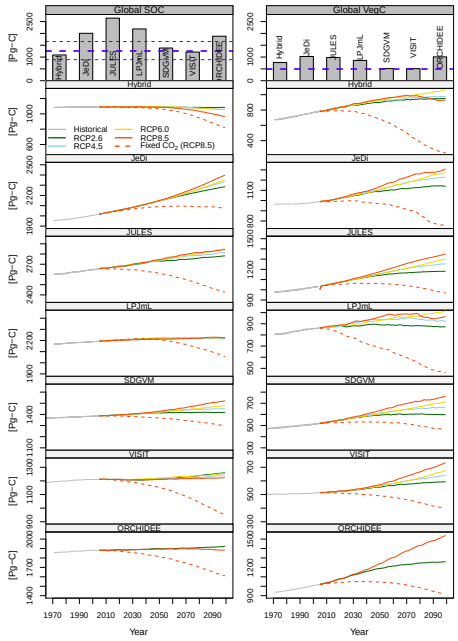

Fig. 2. Changes in global SOC and VegC stocks of each biome model in HadGEM forced by each RCP. Upper bar charts indicate global SOC and VegC stocks in 2000. In the bar chart for global SOC, blue lines indicate the empirical global SOC stock estimated by Todd-Brown et al. (2013) based on Harmonized World Soil Database (solid line indicates mean and dotted lines indicate 95 % confidence intervals). In the bar chart for global VegC, blue line indicates empirical global VegC stock estimated by Ruesch and Gibbs (2008).

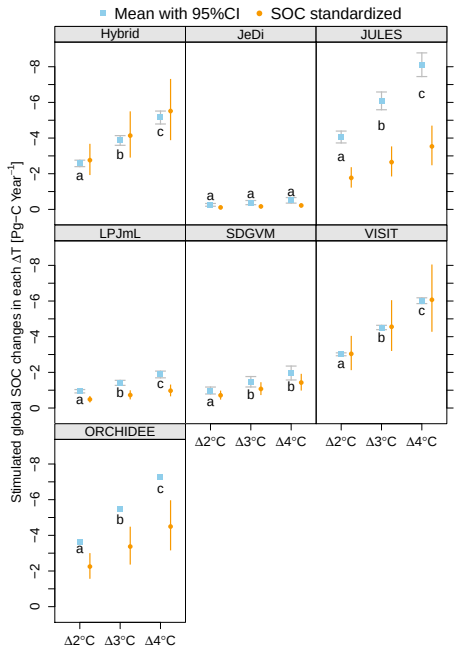

Fig. 3. Estimated global SOC changes in response to each ΔT in each biome model based on the original global SOC stock at 2000 (blue symbols) and standardized as the empirical global SOC stock (1255 Pg C, 95 % C.I.; 891 Pg C–1657 Pg C) estimated in Todd-Brown et al. (2013). Different letters indicate no partial duplication among 95 % CI for each biome model (Table 2).

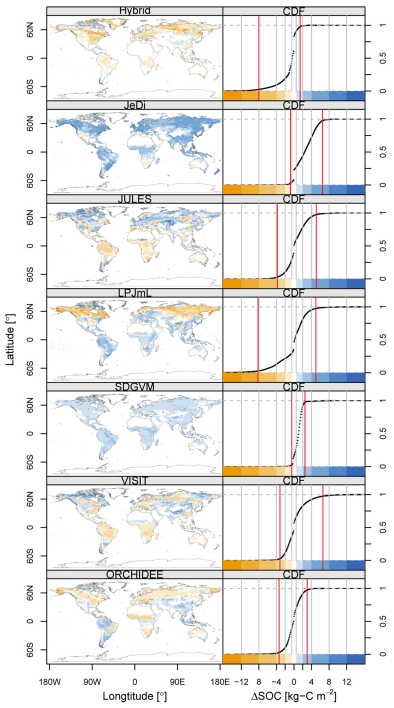

Fig. 4. Maps of SOC changes by 2099 from 2000 and cumulative density function (CDF) in each biome model in HadGEM RCP8.5. In the plot of CDF, red lines indicate 2.5 and 97.5 percentiles of SOC changes.

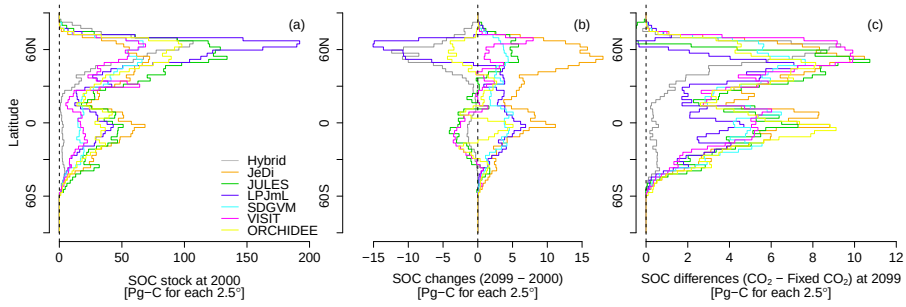

Fig. 5. Latitudinal SOC stocks: **(a)** SOC changes (2099–2000 in RCP8.5); **(b)** indirect CO_2 effect on SOC (CO_2 experiment – Fixed CO_2 experiment at 2099 in RCP8.5); and **(c)** in HadGEM.